Inorganic Chemistry

Article

pubs.acs.org/IC

Aluminum, Gallium, Germanium, Copper, and Phosphorus Complexes of *meso*-Triaryltetrabenzocorrole

Giuseppe Pomarico,[†] Sara Nardis,[†] Mario L. Naitana,[†] M. Graça H. Vicente,[‡] Karl M. Kadish,*[,§] Ping Chen,[§] Luca Prodi,[⊥] Damiano Genovese,[⊥] and Roberto Paolesse*[,†,∥]

[†]Dipartimento di Scienze e Tecnologie Chimiche, Università di Roma Tor Vergata, via della Ricerca Scientifica 1, 00133 Rome, Italy

[‡]Department of Chemistry, Louisiana State University, Baton Rouge, Louisiana 70803, United States

[§]Department of Chemistry, University of Houston, Houston, Texas 77204-5003, United States

[⊥]Department of Chemistry, "G. Ciamician" Università di Bologna, 40126 Bologna, Italy

[∥]CNR IDASC, via Fosso del Cavaliere, 00133 Rome, Italy

Supporting Information

ABSTRACT: 5,10,15-Triaryltetrabenzocorrole complexes of aluminum, gallium, germanium, and phosphorus were synthesized by coordination of these metal ions in the preformed triaryltetrabenzocorrole macrocycle, opening a way to the investigation of different metal complexes. The UV−vis spectra of these derivatives exhibit a red shift and broadening of all absorption bands because of the π-extended aromatic system and distortion of the molecular framework. The electrochemical and photophysical behaviors of the free base and the metal complexes of *meso*-triaryltetrabenzocorrole were investigated and characterized.

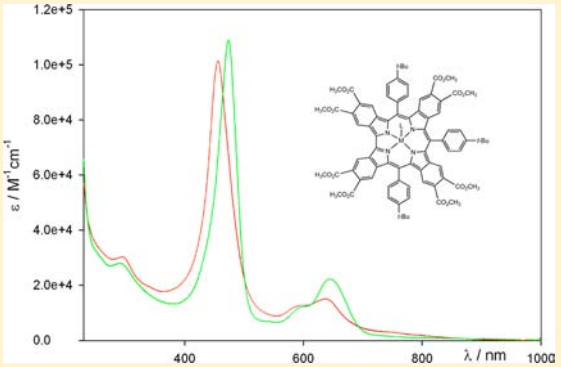

INTRODUCTION

Corroles are contracted porphyrins that are characterized by substitution of a *meso*-carbon with a direct pyrrole−pyrrole link, thus making the molecular skeleton similar to that of corrin, the vitamin B12 nucleus. In the cornucopia of the all porphyrin analogues, corroles have now fully come into the limelight, following the publication of efficient synthetic protocols for the preparation of 5,10,15-triarylcorroles from commercially available precursors.[1,2] The possibility of preparing a wide range of *meso*-triarylcorroles has triggered an exploration of the chemistry of these macrocycles, leading to a better understanding of their reactivity,[3] coordination chemistry,[4,5] and photophysics;[6,7] such a richness of properties has been accompanied by an extensive exploitation of corroles in a number of different applications, both in their free-base form and as corresponding metal complexes.[8]

Studies of corrole chemistry have led to a better understanding of the structure−property relationships, which is a key step in the design of new dyes targeted for different applications. Among the various functionalizations of the porphyrinoid framework, the fusion of benzene or other aromatic moieties onto the β positions of the corrole macrocycle has attracted particular interest because this process results in a significant modification of the compound's optical features, due to expansion of the macrocyclic aromatic π system.

Taking into account the unique optical properties of *meso*-tetraaryltetrabenzoporphyrins,[9,10] we recently investigated the possibility of converting *meso*-triarylcorroles to the corresponding *meso*-triaryltetrabenzocorroles, following two different synthetic methodologies, for the preparation of these macrocycles.[11] As expected, the resulting corrole derivatives show a Soret band that is strongly red-shifted with respect to the parent corrole, making these macrocycles appealing for their use as photosensitizers in medicine or as organic substrates in materials chemistry.[12,13]

The coordination of suitable metal ions can further induce modifications in the corrole optical properties, and the formation of some metal complexes can lead in many cases to an enhancement of the photophysical features of the macrocycle, so that it becomes comparable to or even better than that of the corresponding porphyrin.[5] For this reason, we decided to prepare metal complexes of *meso*-triaryltetrabenzocorroles, with one aim being to investigate the charges resulting from an extended aromatic system combined with coordination of the main-group metal ions. In particular, we chose to prepare aluminum(III),[14] gallium(III),[15] germanium(IV),[16] and phosphorus(V)[17] benzocorrolates, prompted by the exciting results reported when these ions were coordinated to common

Received: January 21, 2013
Published: March 12, 2013

aryl corroles, particularly the intense fluorescence quantum yields observed for these metal derivatives.

In this paper, we report synthetic details for the preparation of these main-group metal complexes along with detailed photophysical, electrochemical, and spectroelectrochemical characterization of the different metal complexes of *meso*-triaryltetrabenzocorrole (Figure 1).

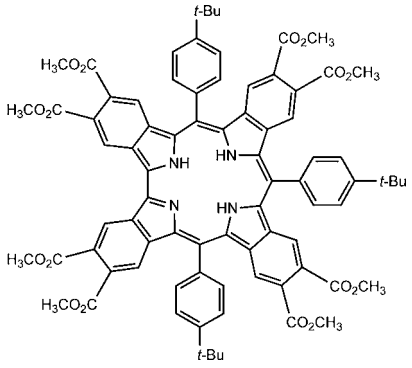

Figure 1. Structure of the investigated free-base triaryltetrabenzocorrole.

EXPERIMENTAL SECTION

Materials. Silica gel 60 (70−230 mesh, Sigma Aldrich) was used for column chromatography. Reagents and solvents (Aldrich, Fluka) were of the highest grade available and were used without further purification. Room temperature ^{1}H and ^{31}P NMR spectra were recorded on a Bruker AV300 spectrometer operating at 300.13 MHz (^{1}H) or 121.48 MHz (^{31}P). Chemical shifts are given in ppm relative to a residual solvent ($CHCl_3$, 7.26 ppm; CH_2Cl_2, 5.32 ppm) for ^{1}H and to a $CDCl_3$ solution of PPh_3 (−6.1 ppm) as the external standard for ^{31}P. Variable-temperature NMR spectra were recorded on a Bruker AV400 spectrometer operating at 400.13 MHz using CD_2Cl_2 as the solvent. Mass spectrometry (MS) spectra (TOF-SIMS) were recorded using a positive method with a TOF-SIMS V (IONTOF) spectrometer. UV−vis spectra were measured in CH_2Cl_2 or toluene with either a Varian Cary 50 or a Perkin-Elmer Lambda 45 spectrophotometer. Quartz cuvettes with optical path length of 1 cm were used. The fluorescence spectra were recorded with an Edinburgh FLS920 equipped Hamamatsu R928P photomultiplier for emission up to 800 nm and with a germanium detector for the 800−1600 nm spectral range. The same instrument connected to a PCS900 PC card was used for the time-correlated single photon counting experiments. Luminescence quantum yields (uncertainty ±15%) were determined using solutions of the tetraphenylporphyin free base in toluene as a reference (Φ = 0.11), and fluorescence intensities were corrected for inner filter effects according to standard methods.[18]

Syntheses of Metallobenzocorroles. [5,10,15-Tris(4-*tert*-butylphenyl)-2:3,7:8,12:13,17:18-tetrabenzo-2″,3″,7″,8″,12″,13″,17″,18″-octakis(carboxymethyl)corrolato]copper ([TBCorr]Cu, **1**) was synthesized following a literature method.[11] 5,10,15-Tris(4-*tert*-butylphenyl)-2:3,7:8,12:13,17:18-tetrabenzo-2″,3″,7″,8″,12″,13″,17″,18″-octakis(carboxymethyl)corrole (TBCorrH$_3$, **2**) was prepared by demetalation of **1** following a published method.[19]

*[5,10,15-Tris(4-tert-butylphenyl)-2:3,7:8,12:13,17:18-tetrabenzo-2″,3″,7″,8″,12″,13″,17″,18″-octakis(carboxymethyl)corrolato]-aluminum(pyridine) ([TBCorr]Al(py), **3**).* To 45 mg of **2** (0.033 mmol) dissolved in 8 mL of toluene was added 90 μL (0.171 mmol) of a 1.9 M solution of $AlEt_3$ in toluene, and the mixture was stirred at room temperature under nitrogen while the course of the reaction was monitored by UV−vis spectroscopy. After 10 min, the reaction mixture was cooled by an ice bath, and 200 μL of water was added to destroy excess $AlEt_3$. A total of 1 mL of pyridine (py) was added, after which the reaction mixture was filtered and the solvent removed by reduced pressure. The preciptate was washed with CH_2Cl_2 and purified by chromatography on silica gel, eluting with tetrahydrofuran (THF)/hexane from 1:2 to 1:1. Fractions containing aluminum corrole were collected, the solvent was removed under vacuum, and the residue was crystallized from CH_2Cl_2/hexane with the addition of a few drops of py. Yield: 56% (27 mg). Mp: >300 °C. UV−vis (toluene): λ_{max}, nm (log ε, M^{-1} cm^{-1}): 474 (4.53), 645 (3.91). ^{1}H NMR (300.13 MHz, $CDCl_3$): δ 7.96−7.34 (m, 20 H, β-fused + phenyls), 4.11−3.34 (m, 24 H, $-CO_2CH_3$), 1.63 (br s, 27 H, *tert*-butyls). Anal. Calcd for $C_{86}H_{76}AlN_5O_{16}$: C, 70.63; H, 5.24; N, 4.79. Found: C, 70.69; H, 5.18 N, 4.83.

*[5,10,15-Tris(4-tert-butylphenyl)-2:3,7:8,12:13,17:18-tetrabenzo-2″,3″,7″,8″,12″,13″,17″,18″-octakis(carboxymethyl)corrolato]-gallium(pyridine) ([TBCorr]Ga(py), **4**).* To 40 mg of **2** (0.029 mmol) dissolved in 20 mL of py was added a large excess of $Ga(acac)_3$, and the mixture was refluxed under nitrogen, monitoring the course of the reaction by UV−vis spectroscopy. After 2 h, the solvent was removed by reduced pressure and the residue purified by chromatography on silica gel, eluting with a gradient THF/hexane from 1:2 to 1:1. Fractions containing gallium corrole were collected, the solvent was removed under vacuum, and the residue was crystallized from CH_2Cl_2/hexane in the presence of a few drops of py. Yield: 66% (29 mg). Mp: >300 °C. UV−vis (toluene): λ_{max}, nm (log ε, M^{-1} cm^{-1}) 478 (4.78), 657 (4.17). ^{1}H NMR (300.13 MHz, $CDCl_3$): δ 8.12−7.34 (m, 20 H, β-fused + phenyls), 4.23−3.31 (m, 24 H, $-CO_2CH_3$), 1.59 (br s, 27 H, *tert*-butyls). MS (TOF-SIMS, *m*/*z*): 1426.1 (M^+ − Py). Anal. Calcd for $C_{86}H_{76}GaN_5O_{16}$: C, 68.62; H, 5.09; N, 4.65. Found: C, 68.69; H, 5.05 N, 4.68.

*[5,10,15-Tris(4-tert-butylphenyl)-2:3,7:8,12:13,17:18-tetrabenzo-2″,3″,7″,8″,12″,13″,17″,18″-octakis(carboxymethyl)corrolato]-germanium(hydroxyl) ([TBCorr]Ge(OH), **5**).* To 40 mg of **2** (0.029 mmol) dissolved in 10 mL of anhydrous *N*,*N*-dimethylformamide (DMF) was added 17 μL (0.15 mmol) of $GeCl_4$, and the mixture was refluxed under nitrogen while the course of the reaction was monitored by UV−vis spectroscopy. After 1.5 h, the solvent was removed and the residue dissolved with CH_2Cl_2 and purified by chromatography on silica gel, eluting with THF/hexane from 1:2 to 1:1. Fractions containing germanium corrole were collected and crystallized from CH_2Cl_2/hexane. Yield: 57% (24 mg). Mp: >300 °C. UV−vis (toluene): λ_{max}, nm (log ε, M^{-1} cm^{-1}) 456 (5.00), 640 (4.18). ^{1}H NMR (300.13 MHz, $CDCl_3$): δ 8.38−7.32 (m, 20 H, β-fused + phenyls), 4.44−3.51 (m, 24 H, $-CO_2CH_3$), 1.66 (br s, 27 H, *tert*-butyls), −3.90 (br s, 1H, axial −OH). MS (TOF-SIMS, *m*/*z*): 1446.46 (M^+). Anal. Calcd for $C_{81}H_{72}GeN_4O_{17}$: C, 67.28; H, 5.02; N, 3.87. Found: C, 67.24; H, 5.06 N, 3.84.

*[5,10,15-Tris(4-tert-butylphenyl)-2:3,7:8,12:13,17:18-tetrabenzo-2″,3″,7″,8″,12″,13″,17″,18″-octakis(carboxymethyl)corrolato]-phosphorus(dihydroxyl) ([TBCorr]P(OH)$_2$, **6**).* To 45 mg of **2** (0.033 mmol) dissolved in 15 mL of py was added 261 μL (2.81 mmol) of $POCl_3$, and the mixture was refluxed under nitrogen while the course of the reaction was monitored by UV−vis spectroscopy. After 1.5 h, the solvent was removed and the residue dissolved with CH_2Cl_2 and purified by chromatography on silica gel, eluting with ethyl acetate/hexane from 1:1 to 2:1. Fractions containing phosphorus corrole were collected, the solvent was removed under reduced pressure, and the residue was crystallized from CH_2Cl_2/hexane. Yield: 36% (17 mg). Mp: >300 °C. UV−vis (toluene): λ_{max}, nm (log ε, M^{-1} cm^{-1}) 474 (5.03), 645 (4.36). ^{1}H NMR (300.13 MHz, $CDCl_3$): δ 8.36−7.47 (m, 20 H, β-fused + phenyls), 4.29−3.34 (m, 24 H, $-CO_2CH_3$), 1.60 (br s, 27 H, *tert*-butyls), −3.26 (br s, 2H, axial −OH). ^{31}P NMR (121.48 MHz, $CDCl_3$): δ −186. MS (TOF-SIMS, *m*/*z*): 1422.95 (M^+). Anal. Calcd for $C_{81}H_{73}N_4O_{18}P$: C, 68.44; H, 5.18; N, 3.94. Found: C, 68.49; H, 5.24; N, 3.91.

Electrochemical and Spectroelectrochemical Measurements. Absolute dichloromethane (CH_2Cl_2; 99.8%, EMD Chemicals Inc.) and pyridine (py; 99.8%, Sigma-Aldrich Chemical Co.) were used for electrochemistry without further purification. Benzonitrile (PhCN) was purchased from Aldrich Chemical Co. and distilled over P_2O_5 under vacuum prior to use. Tetra-*n*-butylammonium perchlorate (TBAP), used as the supporting electrolyte, was purchased from Sigma

dx.doi.org/10.1021/ic400162y | Inorg. Chem. 2013, 52, 4061−4070

Scheme 1. Synthetic Pathway for the Preparation of *meso*-Triaryltetrabenzocorrole Metal Complexes

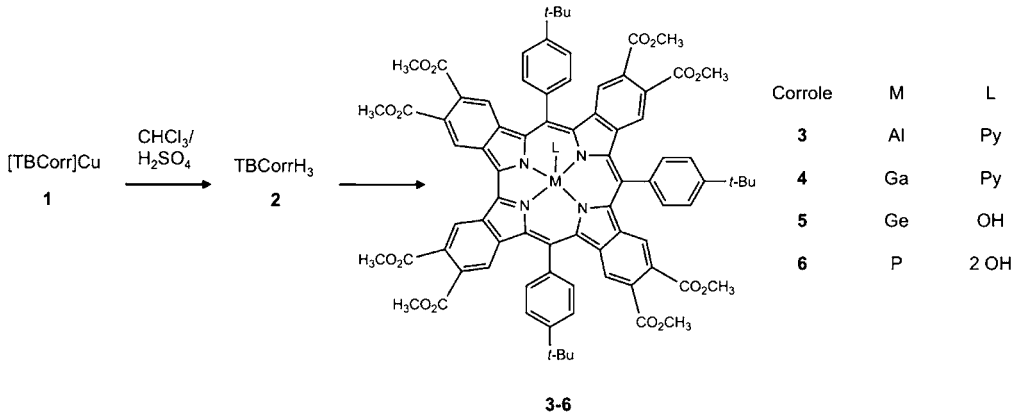

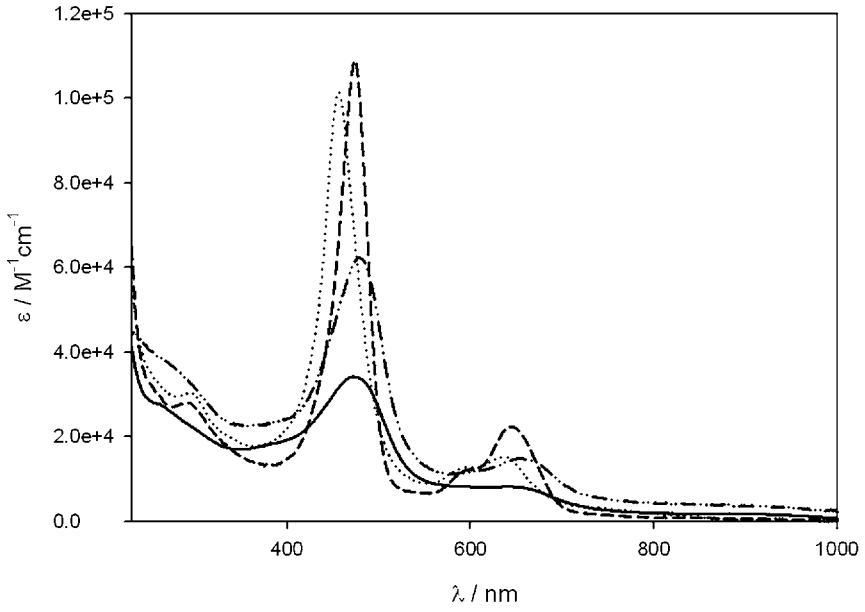

Figure 2. UV−vis absorption spectra of **3** (solid line), **4** (dash-dotted line), **5** (dotted line), and **6** (dashed line).

Chemical Co. or Fluka Chemika Co., recrystallized from ethyl alcohol, and dried under vacuum at 40 °C for at least 1 week prior to use.

Cyclic voltammetry was carried out with an EG&G model 173 potentiostat/galvanostat. A homemade three-electrode electrochemistry cell was used and consisted of a platinum button or a glassy carbon working electrode, a platinum wire counter electrode, and a saturated calomel reference electrode (SCE). The SCE was separated from the bulk of the solution by a fritted-glass bridge of low porosity that contained the solvent/supporting electrolyte mixture. All potentials are referenced to the SCE.

UV−vis spectroelectrochemical experiments were performed with an optically transparent platinum thin-layer electrode of the type described in the literature.[20] Potentials were applied with an EG&G model 173 potentiostat/galvanostat. Time-resolved UV−vis spectra were recorded with a Hewlett-Packard model 8453 diode-array rapid-scanning spectrophotometer.

RESULTS AND DISCUSSION

Synthesis and Characterization. The procedure reported for the preparation of *meso*-triaryltetrabenzocorrole involves a three-step reaction,[11] where the starting material is *meso*-triarylcorrole, which is first metalated with copper and then fully brominated at the β-pyrrole positions of the macrocycle. The halogenated complex undergoes a cross-coupling reaction under Heck conditions with a 100-fold excess of methyl acrylate; the reaction intermediate was not isolated but was further reacted through 6π electrocyclization with aromatization of the fused cyclohexane rings, thus allowing formation of the β-fused benzene rings. This procedure, developed for the preparation of *opp*-dibenzoporphyrins,[21] leads to the formation of *meso*-triaryltetrabenzocorroles in good yield.

Because of the harsh conditions needed for bromination at the macrocycle peripheral positions, the insertion of a copper ion is necessary to protect the macrocycle, limiting its decomposition, which is triggered by an excess of bromine. This procedure can also be used for the preparation of different metal complexes, replacing copper with other metals, thus allowing for formation of the corresponding metallobenzocorroles (Scheme 1).

Among the four investigated metal derivatives, only aluminum[22] and gallium[23] corrolates could undergo octabromination; in the case of germanium corrole, only partially brominated derivatives could be obtained[16] because of a competing ring-opening reaction that occurred when complete bromination was attempted. This particular behavior can be attributed to the Ge^{IV} oxidation state, with the higher positive charge acting to withdraw the electron density from the

dx.doi.org/10.1021/ic400162y | Inorg. Chem. 2013, 52, 4061−4070

macrocycle, thus deactivating the peripheral positions and hindering formation of fully brominated germanium corrole. A similar behavior was also expected to occur in the case of phosphorus corrole because of the positive charge of the phosphorus(V)-coordinated species.

The limited scope of the complete bromination reaction of metallocorroles for the subsequent preparation of corresponding tetrabenzocorroles could, however, be easily circumvented by using a different approach, as shown in Scheme 1. Following the preparation of copper tetrabenzocorrole **1**, the metal ion was removed by a procedure reported for demetalation of corrole complexes,[19] leading to isolation of **2**. The free-base compound was then further reacted to prepare the desired metallocorrole derivatives, following a successful approach earlier reported for the preparation of cobalt and tin tetrabenzocorroles.[11]

Compound **3** was prepared by reacting **2**, dissolved in toluene, with a 1.9 M $AlEt_3$/toluene solution at room temperature, under an inert atmosphere. The reaction proceeds quickly, and complete variation of the UV−vis spectrum was observed after 10 min. The reaction workup yielded **3**, as the corresponding pyridino derivative.

The number of py moieties coordinated to aluminum(III) arylcorrolates has recently been clarified.[25] This metal may form a penta- or hexacoordinated species, depending upon the solvent medium; the pentacoordinated form is observed when the complex is dissolved in a noncoordinating solvent, while the addition of different volumes of py to the solvent generates an equilibrium between the penta- and hexacoordinated species, with the latter obtained in neat py. The UV−vis spectrum of **3** recorded in a noncoordinating solvent, such as toluene and CH_2Cl_2 (Figure 2), showed a Soret band at 474 nm and a Q band at 645 nm, which is 43 nm red-shifted compared with that of **1**; in the presence of excess py, the spectrum became broad in the Q-band region as the hexacoordinated species is formed.

Compound **4** was obtained by refluxing the free-base benzocorrole in py, containing an excess of $Ga(acac)_3$; after 2 h, the UV−vis spectrum of the reaction mixture showed complete disappearance of the starting material. The reaction workup yielded the final complex with py as an axial ligand; the UV−vis spectrum of this compound is very similar to that of **3**, with a Soret band at 478 nm and a weaker absorbance at 657 nm (Figure 2); a further change in the spectrum due to formation of the hexacoordinated complex was observed when **4** was dissolved in neat py, with a broadening of the Q band, while a similar variation in the spectrum of **3** occurs in a 1:1 mixture of CH_2Cl_2/py.

The ^{1}H NMR spectra of **3** and **4**, recorded at room temperature, show three main groups of unresolved signals related to the aromatic protons of the *meso*-phenyl and *β*-fused benzene rings, (7.96−7.34 ppm for **3** and 8.12−7.34 ppm for **4**); the second group of signals (4.11−3.33 ppm for **3** and 4.23−3.31 ppm for **4**) belong to the carboxymethyl substituents, while the *tert*-butyl groups appear as a broad singlet centered at 1.63 ppm for **3** and at 1.51 ppm for **4** (see Figures S1 and S2 in the Supporting Information, SI).

For the preparation of **5**, the free base **2** was dissolved in anhydrous DMF under an inert atmosphere, after which $GeCl_4$ was added and the resulting mixture stirred under reflux and under N_2 for 2 h. A chloro complex was initially obtained, but this quickly hydrolyzed, leading to formation of the Ge−OH derivative. The lability of the initially formed Ge−Cl adduct was confirmed by ^{1}H NMR analysis; in addition to the three groups of expected signals for **5** (aromatic, 8.38−7.32 ppm; carboxymethyl, 4.44−3.51 ppm; *tert*-butyl, broad singlet at 1.66 ppm), a broad signal at −3.9 ppm was observed due to the hydroxyl group, which is axially bound to germanium (Figure S3 in the SI). Narrower absorption bands are seen in the UV−vis spectrum and the Soret and Q bands appear at 456 and at 640 nm, respectively, with a blue-shifted shoulder for the Q band (Figure 2). The high values measured in both the absorption and emission spectra (see the later sections) seem to indicate a less distorted geometry for **5** than those of complexes **3** and **4**.

The series of *meso*-triaryltetrabenzocorrole complexes was completed by the insertion of phosphorus. Free base **2** was dissolved in py, and an 85-fold excess of $POCl_3$ was added. The mixture was stirred under reflux and a N_2 atmosphere for 90 min. The reaction workup yielded a phosphorus complex with two axially bound hydroxyl units.

The spectroscopic properties of **6** are similar to those of **5**. The UV−vis spectrum exhibits a Soret band at 474 nm and a Q band at 645 nm, with a blue-shifted shoulder (Figure 2). Large absorbance and emission values are obtained (see the photophysical characterization in a later section), which suggests a deviation from planarity of the macrocycle similar to that of **5** but less pronounced with respect to the aluminum and gallium complexes.

The ^{1}H NMR spectrum of phosphorus corrole is very similar to that of other metal complexes for the aromatic (8.36−7.47 ppm), carboxymethyl (4.29−3.34 ppm), and *tert*-butyl (broad singlet at 1.60 ppm) protons, while the inner −OH groups appear as a broad signal at −3.26 ppm (Figure S4 in the SI). The behavior of the coordinated phosphorus ion toward axial ligands was investigated by attempting to replace OH^- with OCH_3^- by stirring the phosphorus complex in methanol for 72 h. While no variations were seen in the UV−vis spectrum, the ^{1}H NMR spectrum showed the presence of two doublets of different intensities, with J = 24 Hz (because of the P−OCH_3 coupling) at −1.52 and −1.87 ppm (Figure S5 in the SI). These doublets did not completely replace the broad signal of the inner OH, thus confirming the large affinity toward the hydroxyl groups (in the case of phosphorus triarylcorrole, the complete conversion of hydroxy into a methoxy derivative occurred after the addition of 125 equiv of methanol to the NMR tube[17]).

Another peculiarity reported for phosphorus corrole[17] is the presence of an equilibrium between the penta- and hexacoordinated species. To identify the predominant form of **6** in solution, we recorded the ^{31}P NMR spectrum. The chemical shifts of the phosphorus nucleus in ^{31}P NMR spectroscopy are sensitive to the coordination number of the phosphorus center.[26] When the phosphorus nucleus is coordinated to a porphyrin, phthalocyanine, or a related macrocycle, it shows signals in the −180/−200 ppm region if it exists in the hexacoordinated form, while evidence of pentacoordination is given by a signal in the range −90 to −110 ppm.

The ^{31}P NMR spectrum of the investigated compound shows a signal at −186 ppm, but no resonances are seen in the range of −90 to −110 ppm; this result indicates that the hexacoordinated form is very stable and is not prone to dissociation to form the pentacoordinated complex. There is also overlap of several signals instead of just a single resonance, as occurs for phosphorus triarylcorroles,[25] thus suggesting the presence of different conformers. A second signal at −170 ppm

dx.doi.org/10.1021/ic400162y | Inorg. Chem. 2013, 52, 4061−4070

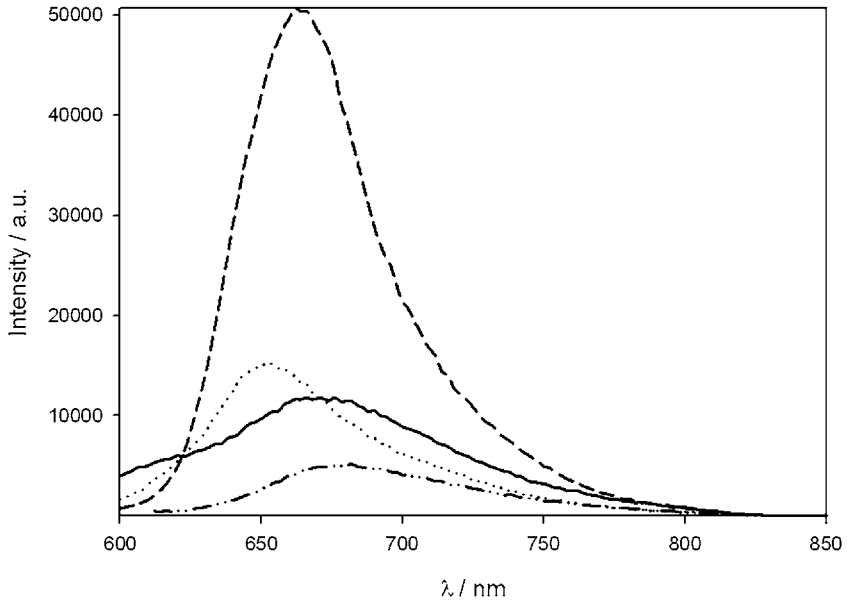

Figure 3. Emission spectra of **3** (solid line), **4** (dash-dotted line), **5** (dotted line), and **6** (dashed line) benzocorrolates.

Table 1. Photophysical Properties of Metallotetrabenzocorrolates in Toluene at Room Temperature

	λ_{absx}, nm	ε, M^{-1} cm^{-1}	λ_{em}, nm	Φ	t, ns	k_r, s^{-1}	k_{nr}, s^{-1}
3	474	34100	670[a]	0.025[b]	1.2	2.1×10^7	8.1×10^8
	645	8200					
4	478	61000	679	0.012	2.9	4.1×10^6	3.40×10^8
	657	14800					
5	456	101000	652	0.042	0.9	4.7×10^7	1.1×10^9
	640	15000					
6	474	108500	665	0.31	3.1	1.0×10^8	2.2×10^8
	645	22800					

[a]Dual emission; see the text. [b]Upon excitation in the Soret band.

in the ^{31}P NMR spectrum was obtained when ligand exchange was attempted, again demonstrating the incomplete ligand substitution (Figure S6 in the SI).

One general feature characteristic of the ^1H NMR spectra for these benzocorrole derivatives is the low resolution of the spectral signals, especially in the aromatic region. This is similar to what was previously reported for the free base and copper complex.[11]

Studies carried out on porphyrins bearing substituents at either the *meso*- or *β*-pyrrole positions suggested the presence of conformers originating from the hampered rotation of phenyls due to crowding of the macrocycle periphery and an inversion of the saddle-shaped porphyrin macrocycle.[27−29]

Unfortunately, we were not able to obtain crystals suitable for X-ray analysis, which would have provided additional information about the geometry of tetrabenzocorroles. However, we can reasonably assume the presence of dynamic processes due to macrocyclic distortions; from this point of view, we tried to further characterize these compounds by investigating their NMR behavior at variable temperature (Figure S7−S9 in the SI). ^1H NMR spectra were recorded at 273, 248, and 223 K with the aim of obtaining better resolved spectra. We chose the **2**, **4**, and **5** derivatives for these studies, with the last two compounds being selected as models for complexes with a neutral or an anionic ligand.

Despite lowering of the temperature, no significant variation of the spectra was observed and an increase of resolution was not observed in the aromatic region of the spectrum, which has the lowest resolution. The only exception was detected with **4**; at −50 °C, the broad signal for the *tert*-butyl substituents was replaced by several signals in the region 1.77−1.51 ppm, suggesting once again the presence of different conformations (Figure S8 in the SI).

These spectroscopic data corroborate the hypothesis of considerable distortion of these complexes: the weak absorbances shown in the UV−vis spectra and the impossibility to observe signals of coordinated py in the ^1H NMR spectra are in agreement with a strong deviation from planarity and with the presence of dynamic processes involving these compounds, which makes ligand exchange very fast and therefore not observable within the NMR time scale. The affinity of metals coordinated to tetrapyrrolic macrocycles toward axial ligands decreases as distortion of the tetrapyrrolic ring increases.

Photophysical Characterization. In general, from the point of view of their photophysical properties, the metallocorroles reported in this manuscript can be divided into two subgroups.

As far as the absorption spectrum is concerned, **5** and **6** show a very intense Soret-like band centered at 456 and 474 nm, respectively, in both dichloromethane and toluene solutions (ε = 101000 and 108500 M^{-1} cm^{-1}). They also show a Q-like set of broader, less intense bands with maxima at 640 and 645 nm, respectively (ε = 15000 and 22800 M^{-1} cm^{-1}; see Figure 2).

dx.doi.org/10.1021/ic400162y | Inorg. Chem. 2013, 52, 4061−4070

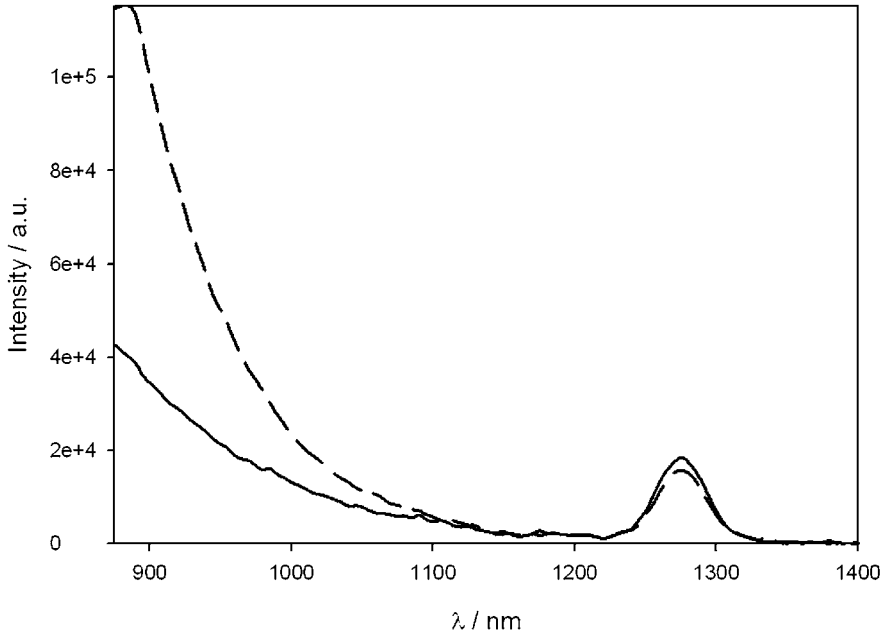

Figure 4. Near-IR emission spectra of **5** (dashed line) and **6** (solid line).

The absorption spectra of **3** and **4** show similar bands, although they are much broader and less intense (ε_{max} = 34100 and 61000 M^{-1} cm^{-1}). The fluorescence spectra show even larger differences. In particular, **5** and **6** show at room temperature an unstructured band in the red region, with a rather short excited-state lifetime (see Figure 3 and Table 1). These two corroles present rather high emission quantum yields, with the data for **6** being remarkably high (31%). Overall, its photophysical properties confer to **6** a very high brightness, comparable to that shown by most currently used dyes, including derivatives of BODIPYs, xanthones, and cyanines.

For these two macrocycles, the excitation spectrum is proportional to the absorption spectrum, indicating that the fluorescent excited state is also formed regardless of the excitation wavelength. Similar results were observed at 77 K.

For **5** and **6**, no emission was observed in the 800−1600 nm region either at room temperature or at 77 K, indicating a negligible efficiency for phosphorescence under all experimental conditions. However, an emission peak centered at 1270 nm at room temperature was observed (Figure 4), indicating singlet oxygen sensitization. The excitation spectrum of the singlet oxygen emission matches the absorption bands of the corroles, providing experimental proof of the sensitization mechanism.

The corroles **3** and **4** showed less intense fluorescence at room temperature. Analysis of the excited-state kinetics shows that this is due to both a lower radiation rate constant and a faster nonradiatiave process compared to **6** (Table 1). The lower intensities in the absorption spectra are in agreement with these data, suggesting a greater distortion of the macrocycle skeleton in the case of the **3** and **4** complexes. This distortion could also be a reason for the lack of singlet oxygen sensitization observed for these two complexes, which would require longer triplet-state lifetimes.

Electrochemistry and Spectroelectrochemistry. The electrochemical and UV−vis properties of compounds **1**−**6** were examined before and after oxidation/reduction in CH_2Cl_2, PhCN, and py. The measured half-wave or peak potentials are summarized in Table 2, which includes literature data for related triaryl- and octaethylcorroles under the same solution conditions. Cyclic voltammograms of **1**, **3**, and **4** in the three utilized solvents are illustrated in Figures 5 and 6, while cyclic voltammograms of **2**, **5**, and **6** are given in the Supporting Information (Figures S13−S15).

The most well-defined electrochemistry occurs for the copper derivative **1**, which exhibits two reversible oxidations and three reversible reductions in PhCN and CH_2Cl_2, containing 0.1 M TBAP. A second reversible oxidation cannot be observed in py because of the limited positive potential window of this solvent.

Both oxidations of copper corrole are assigned as macrocycle-centered because the Cu^{III} central metal ion cannot be further oxidized and the eight electron-withdrawing ester groups (CO_2Me) on the macrocycle should also not be oxidized in the investigated range of potentials.

In contrast to copper(III) corrole, multiple oxidation processes are observed for aluminum(III) corrole **3** and gallium(III) corrole **4** in CH_2Cl_2 and PhCN, while only two oxidations are seen for the same corroles in py, which has a smaller positive potential window. The py axial ligand in **3** and **4** can be replaced by a ClO_4^- anion from the supporting electrolyte after oxidation, and PhCN can also axially bind to the central metal ion before or after oxidation, which might give different ligated forms of each corrole in solution, each of which might have a different half-wave potential. However, the fact that the two oxidations of **3** and **4** seem to be split into four processes in CH_2Cl_2 or PhCN suggests that the py ligand is dissociated in CH_2Cl_2 and PhCN, inducing the probable formation of a $\pi-\pi$ dimer with two equivalent redox centers. A similar oxidation behavior is seen for germanium(IV) corrole (see Table 2 and Figure S14 in the SI) in that the two oxidations are split into four processes in the nonbinding solvent CH_2Cl_2, but only two oxidations are observed in PhCN, the more strongly coordinating solvent.

The first reduction of **1** is assigned to the Cu^{III}/Cu^{II} process, as has been reported for a large number of copper(III) corroles

dx.doi.org/10.1021/ic400162y | Inorg. Chem. 2013, 52, 4061−4070

Table 2. Half-Wave and Peak Potentials (V vs SCE) of the Investigated *meso*-Triaryltetrabenzocorrole Complexes in CH_2Cl_2, PhCN, and py (0.1 M TBAP at a Scan Rate of 0.1 V s^{-1})

				oxidation		reduction				
compd		compd no.	solvent	second ring	first ring	Cu^{III}/Cu^{II}	side reactions	benzo-CO_2Me	first ring	ref[a]
copper series	[TBCorr]Cu	**1**	CH_2Cl_2	1.38	0.82	0.07		−1.38	−1.59	tw
			PhCN	1.39	0.80	0.06		−1.42	−1.62	tw
			py		0.71	0.11		−1.33	−1.55	tw
	[Br_8TTCorr]Cu		CH_2Cl_2	1.64	1.13	0.08			−1.62[b]	30
	[TTCorr]Cu			1.35	0.70	−0.23				30
	[TPCorr]Cu			1.37	0.78	−0.19				30
	[OECorr]Cu			1.14	0.57, 0.43	−0.34				31
free base	[TBCorr]H_3	**2**	CH_2Cl_2	0.68, 0.57[b]	0.12[c]		−0.72[d]	−1.32	−1.56	tw
			PhCN	0.83, 0.58[b]	0.18[c]		−0.58[d]	−1.30	−1.50	tw
			py	0.70	0.21		−0.59[d]	−1.30	−1.51	tw
	[TTCorr]H_3		py	0.56[b]	0.09		−1.33[d]		−1.88	32
aluminum and gallium series	[TBCorr]Al(py)	**3**	CH_2Cl_2	0.95, 0.73	0.43, 0.29			−1.35	−1.55	tw
			PhCN	1.02, 0.75	0.47, 0.28			−1.33	−1.56	tw
			py	0.82	0.38			−1.27	−1.52	tw
	[TBCorr]Ga(py)	**4**	CH_2Cl_2	1.25, 0.92	0.57, 0.16			−1.25	−1.48	tw
			PhCN	1.27, 0.93	0.58, 0.14			−1.28	−1.52	tw
			py	0.95, 0.73	0.43, 0.29			−1.25	−1.50	tw
	[T(C_6F_5)Corr]Ga(py)				0.75					15
germanium series	[TBCorr]Ge(OH)	**5**	CH_2Cl_2	1.23, 1.13	0.92, 0.78		−0.71,[e] −1.10[e]	−1.35	−1.55	tw
			PhCN	1.27	0.90		−0.69,[e] −1.10[e]	−1.40[b]	−1.58	tw
			py		0.78		−0.65,[e] −1.10[e]	−1.48[b]	−1.63	tw
	[T(C_6F_5)Corr]Ge(OH)		CH_2Cl_2		1.13					33
phosphorus series	[TBCorr]$P(OH)_2$	**6**	CH_2Cl_2	1.35, 1.18	0.74		0.11,[e] −0.65,[e] −0.81,[e] −1.05[e]	−1.33	−1.54	tw
			PhCN	1.34, 1.17	0.75		0.07,[e] −0.66,[e] −0.85,[e] −1.08[e]	−1.35	−1.56	tw
			py		0.76		0.20,[e] −0.55,[e] −0.78,[e] −1.02[e]	−1.29	−1.50	tw
	[TPCorr]$P(OH)_2$		CH_3CN	1.22	0.72				−1.41	17
	[OECorr])P(O)		PhCN	1.17[b]	0.80				−1.58	34

[a]tw = this work. [b]Peak potential. [c]This redox couple can only be seen on the second positive potential sweep after scanning through the first reduction. [d]Irreversible deprotonation process. [e]Unknown process with minor current, and most are irreversible.

in nonaqueous media.[30,31,35] Examples of UV−vis spectral changes obtained during this first reduction in a thin-layer cell are shown Figure 7a and are consistent with this assignment.[30,35]

Copper(II) corrole also exhibits two closely spaced reversible reductions after the first metal-centered process. Only one ring-centered reduction is generally observed in this potential region for most corroles without a redox-active central metal ion and also without an extended π-ring system (see Table 2), but the other investigated benzocorrole complexes also exhibit two reductions in the three utilized solvents. On the basis of spectral changes obtained in each controlled reduction of **1** (see Figure 7a), the second reduction is assigned to occur at the electron-withdrawing ester groups (CO_2Me), while the third reduction is assigned as being macrocycle-centered.

Figure 7 compares the spectral changes of **1** and **3** during controlled potential reduction in PhCN containing 0.2 M TBAP. As mentioned above, the spectral changes of **1** upon reduction at −0.20 V in the thin-layer cell are consistent with a metal-centered redox process (see the top set of spectral changes in Figure 7a). Only minimal changes are observed for copper(II) corrole after the potential is switched from −0.20 to −1.55 V (the second reduction), and these changes are illustrated in Figure 7a. This electron addition is proposed to occur at one of the fused benzene rings of the compound containing the electron-withdrawing ester groups (CO_2Me), and this fused benzene ring does not participate in the conjugated system of the macrocycle. Ester groups attached to a benzene ring can undergo one-electron or multielectron reductions,[36] and similar "extra" reductions have also been observed for some ring-expanded porphyrins with CO_2R groups.[37]

Finally, switching the applied potential from −1.55 to −1.75 V leads to a decrease in the intensity of the Soret (500 nm) and

dx.doi.org/10.1021/ic400162y | Inorg. Chem. 2013, 52, 4061−4070

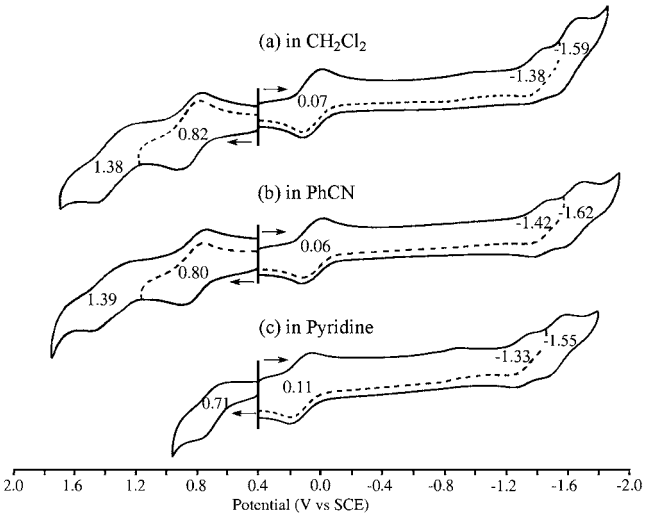

Figure 5. Cyclic voltammograms of copper(III) corrole **1** in (a) CH_2Cl_2, (b) PhCN, and (c) py containing 0.1 M TBAP.

Q (660 nm) bands of copper corrole, and a new broad band then appears at 783 nm, consistent with a macrocycle-centered reaction. Almost identical spectral changes are seen during the two controlled potential reductions of aluminum(III) corrole at −1.45 V and then −1.70 V (Figure 7b), and it is therefore suggested that **1** and **3** both undergo similar reduction mechanisms.

We previously investigated a series of platinum(II) porphyrins with different π-expanded macrocycles[37] and demonstrated that ring expansion of these compounds resulted in a considerable raising of the highest occupied molecular orbital (HOMO) levels, with only a small effect on the lowest unoccupied molecular orbital (LUMO) levels. Because the ring oxidation becomes easier with extended π conjugation and there is only a small effect on the reduction, the HOMO−LUMO gap decreased as the size of the π-conjugated system increased. This is also the case for the ring-expanded corroles. For example, compound **1** and the copper complex of β-octabromo-*meso*-tritolylcorrole [$(Br_8TTCorr)Cu$; see Table 2] both have multiple electron-withdrawing groups on the macrocycle, and the substituent effect of these groups on the redox potentials should be considered as similar. The first metal-centered and first ring-centered reductions of compound **1** and $(Br_8TTCorr)Cu$ are similar to each other, but the potentials for oxidation of the two corroles differ by 260−310 mV. Compound **1**, with a ring-expanded macrocycle, is easier to oxidize.

Electrochemical and spectroelectrochemical data of the ring-expanded free-base corrole **2** suggest that the electrochemical behavior of **2** is similar to that of the "regular" free-base corrole (see Table 2 and Figures S13 and S16 in the SI). First of all, free-base corroles can be easily protonated and/or deprotonated in nonaqueous media to give a mixture of the neutral corrole along with either its protonated, $[(Corr)H_4]^+$, or deprotonated, $[(Corr)H_2]^-$, form in solution.[32,38,39] Protonation and/or deprotonation of free-base corroles is solvent-dependent. As shown in Table 2 and Figure S13 in the SI, the first reduction of **2** is irreversible in all three solvents and located in a range of potentials between −0.59 and −0.72 V for a scan rate of 0.1 V s^{-1}. This reduction is coupled with a loss of one proton from the central nitrogen atoms, giving $[(Corr)H_2]^-$. A similar deprotonation occurs for free-base tritolylcorrole $(TTCorrH_3)$[32] in py, with the difference of the redox potentials between the two compounds being due to the different substituents on the macrocycle. A spectrum assigned to $[(Corr)H_2]^-$ is obtained by Spectroelectrochemisty in the case of the reduced ring-expanded free-base corrole **2**, which is characterized by an intense Soret band at 496−500 nm and two visible bands at 656−717 nm, with the exact value depending on the solvent.

The free-base corrole **2** also undergoes one or two reversible (or quasi-reversible) oxidations at potentials between 0.12 and 0.83 V for a scan rate of 0.1 V s^{-1}. For example, the first oxidation of **2** is located at $E_{1/2}$ = 0.21 V in py. This process is only observed in CH_2Cl_2 and PhCN, after reversal of the initial negative scan at a potential negative of the first reduction and then scanning in a positive direction. The oxidation that results

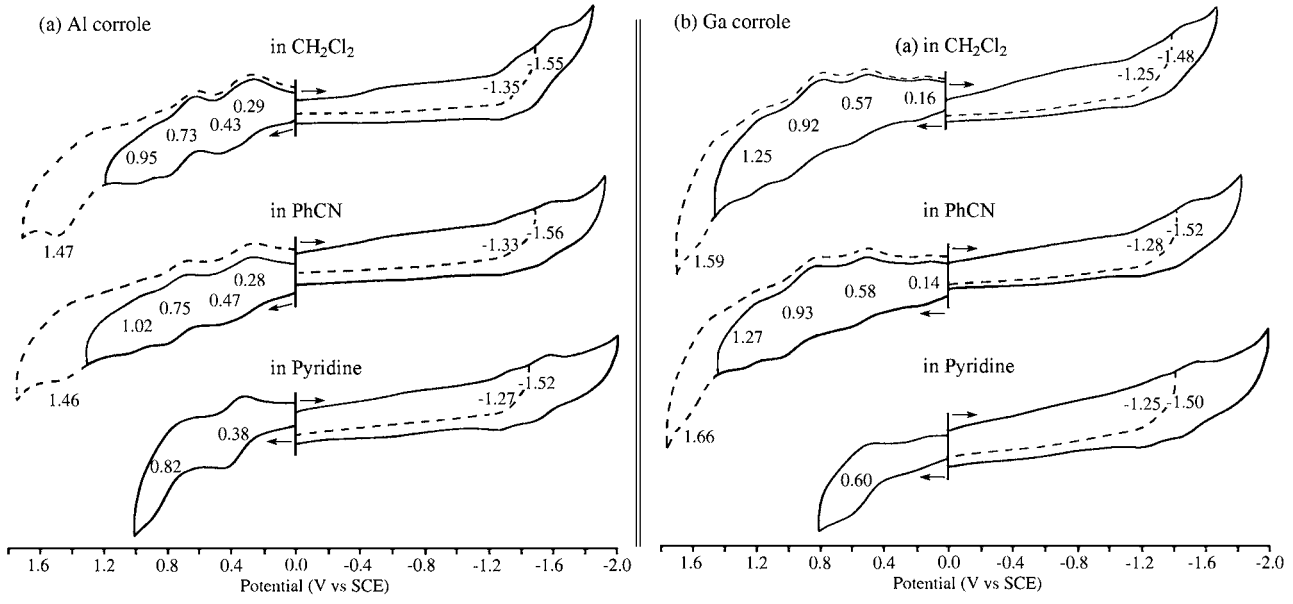

Figure 6. Cyclic voltammograms of (a) **3** and (b) **4** in CH_2Cl_2, PhCN, and py containing 0.1 M TBAP.

dx.doi.org/10.1021/ic400162y | *Inorg. Chem.* 2013, 52, 4061−4070

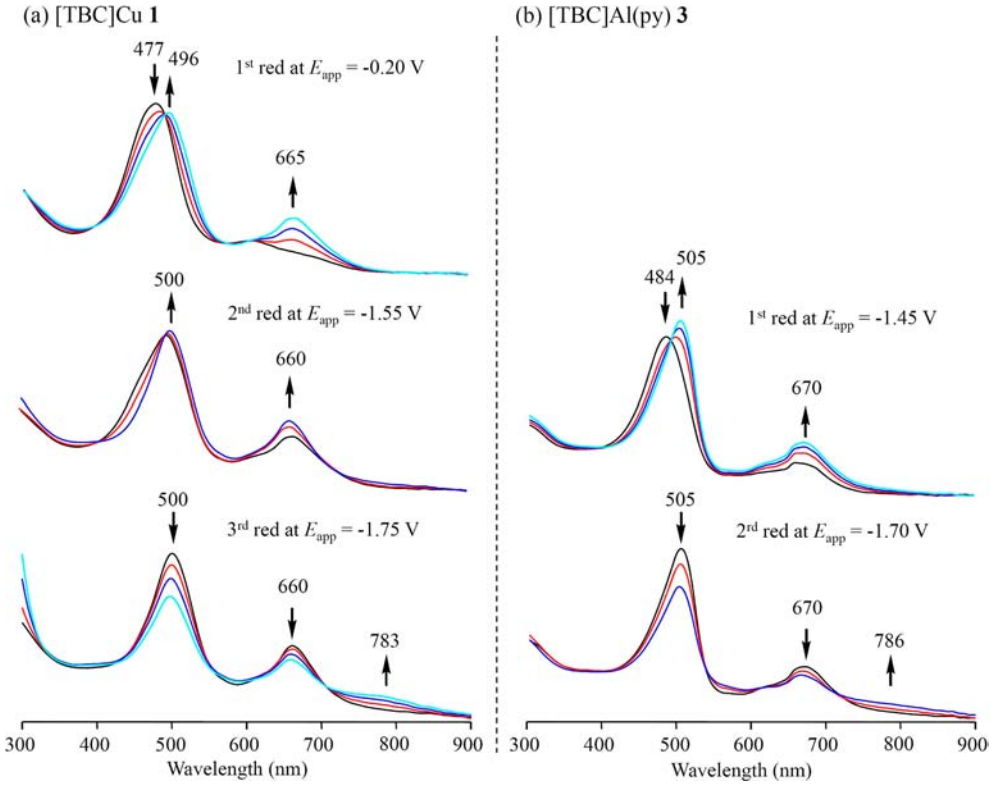

Figure 7. Thin-layer UV−vis spectral changes of (a) **1** and (b) **3** in PhCN containing 0.2 M TBAP during the indicated reductions.

under these experimental conditions involves the $[(Corr)H_2]^-/(^{\bullet}Corr)H_2)$ process.

The redox-active species is assigned as $(Cor)H_3$ in PhCN or CH_2Cl_2 and $[(Corr)H_2]^-$ in the basic py solvent, where one of the three central protons has been lost.[39] In addition to the $[(Corr)H_2]^-/(^{\bullet}Corr)H_2)$ reaction of **2**, another quasi-reversible oxidation is seen at $E_{1/2}$ = 0.70 V in py. This oxidation is separated into two processes in CH_2Cl_2 and PhCN (at 0.57−0.83 V for a scan rate of 0.1 V s^{-1}). Similar to that proposed in earlier studies of other free-base corroles, the oxidation of **2** is proposed to generate a mixture of the free-base neutral corrole radical, $(^{\bullet}Corr)H_2$, and the protonated corrole monocation, $[(Corr)H_4]^+$.[32,39] The final UV−vis spectrum of **2** obtained under controlled potential oxidizing conditions is given in Figure S16 in the SI.

The reductions of [TBCorr]Ge **5** and [TBCorr]P **6** are both ill-defined (Figures S14 and S15 in the SI), and three to four unknown side reactions appear in the potential region of +0.20 to −1.10 V, under the given experimental conditions. These unidentified reactions are currently under continued investigation. The proposed electron-transfer sites for other redox reactions are given in Table 2.

CONCLUSIONS

Tetrabenzocorrole represents an interesting example of the corrole aromatic π-system expansion, operated by the fusion of benzene rings at the peripheral pyrrole β positions of the macrocycle. These derivatives can be obtained by a three-step procedure, which involves the preparation of the copper complex **2** as the starting tetrabenzocorrole derivative. This complex can be demetalated to obtain the corresponding free base, opening the way to the preparation and investigation of different metal derivatives. The electrochemical characterization of these tetrabenzocorrole metal complexes demonstrated a HOMO−LUMO gap decrease, as a consequence of the π-conjugated system expansion, while the photophysical characterization showed large values measured for the fluorescence and singlet oxygen sensitization of these complexes, which were particularly high in the case of the phosphorus derivative. Because the peripheral methyl ester groups can be hydrolyzed to make this derivative water-soluble, these features make this compound particularly promising for PDT and imaging applications, considering that further optimization of triaryltetrabenzocorroles may be obtained by the introduction of suitable substituents on fused benzene rings. These studies are currently in progress in our laboratories.

ASSOCIATED CONTENT

Supporting Information

NMR spectra of **3**−**6**, MS spectra of compounds **4**−**6**, cyclic voltammograms of **2**, **5**, and **6**, and UV−vis spectral changes of **2** during the applied potentials. This material is available free of charge via the Internet at http://pubs.acs.org.

AUTHOR INFORMATION

Corresponding Author

*E-mail: kadish@central.uh.edu (K.M.K.), roberto.paolesse@uniroma2.it (R.P.).

Notes

The authors declare no competing financial interest.

ACKNOWLEDGMENTS

The authors thank the Italian MIUR (to R.P. and L.P., PRIN2009 project 2009Z9ASCA) and the Robert A. Welch Foundation (to K.M.K., Grant E-680) for financial support.

The authors thank Fondazione Roma Dr. Luca Tortora (Tor Vergata University) for recording the MS spectra.

DEDICATION

Dedicated to Professor Maurizio Prato on the occasion of his 60th birthday.

REFERENCES

(1) Paolesse, R.; Jaquinod, L.; Nurco, D. J.; Mini, S.; Sagone, F.; Boschi, T.; Smith, K. M. *Chem. Commun.* **1999**, 1307−1308.
(2) Gross, Z.; Galili, N.; Saltsman, I. *Angew. Chem., Int. Ed.* **1999**, *38*, 1427−1429.
(3) Paolesse, R. *Synlett* **2008**, *15*, 2215−2230.
(4) Erben, C.; Will, S.; Kadish, K. M. In *The Porphyrin Handbook*; Kadish, K. M., Smith, K. M., Guilard, R., Eds.; Academic Press: New York, 2000; Vol. *2*, pp 233−300.
(5) Aviv-Harel, I.; Gross, Z. *Coord. Chem. Rev.* **2011**, *255*, 717−763.
(6) Ding, T.; Alemán, E. A.; Modarelli, D. A.; Ziegler, C. J. *J. Phys. Chem. A* **2005**, *109*, 7411−7417.
(7) Ventura, B.; Degli Esposti, A.; Koszarna, B.; Gryko, D. T.; Flamigni, L. *New J. Chem.* **2005**, *29*, 1559−1566.
(8) Aviv-Harel, I.; Gross, Z. *Chem.—Eur. J.* **2009**, *15*, 8382−8394.
(9) Lash, T. D. *J. Porphyrins Phthalocyanines* **2001**, *5*, 267−288.
(10) Lebedev, A. Y.; Filatov, M. A.; Cheprakov, A. V.; Vinogradov, S. A. *J. Phys. Chem. A* **2008**, *112*, 7723−7733.
(11) Pomarico, G.; Nardis, S.; Paolesse, R.; Ongayi, O. C.; Courtney, B. H.; Fronczek, F. R.; Vicente, M. G. H. *J. Org. Chem.* **2011**, *76*, 3765−3773.
(12) Pandey, R. K.; Zheng, G. In *The Porphyrin Handbook*; Kadish, K. M., Smith, K. M., Guilard, R., Eds.; Academic Press: San Diego, CA, 2000; Vol. *6*, pp 157−230.
(13) Hoffman, B. M.; Ibers, J. A. *Acc. Chem. Res.* **1983**, *16*, 15−21.
(14) Mahammed, A.; Gross, Z. *J. Inorg. Biochem.* **2002**, *88*, 305−309.
(15) Bendix, J.; Dmochowski, I. J.; Gray, H. B.; Mahammed, A.; Simkhovich, L.; Gross, Z. *Angew. Chem., Int. Ed.* **2000**, *39*, 4048−4051.
(16) Nardis, S.; Mandoj, F.; Paolesse, R.; Fronczek, F. R.; Smith, K. M.; Prodi, L.; Montalti, M.; Battistini, G. *Eur. J. Inorg. Chem.* **2007**, 2345−2352.
(17) Ghosh, A.; Ravikanth, M. *Chem.—Eur. J.* **2012**, *18*, 6386−6396.
(18) Montalti, M.; Credi, C.; Prodi, L.; Gandolfi, M. T. *Handbook of Photochemistry*; CRC Press: Boca Raton, FL, 2006.
(19) Mandoj, F.; Nardis, S.; Pomarico, G.; Paolesse, R. *J. Porphyrins Phthalocyanines* **2008**, *12*, 19−26.
(20) Lin, X. Q.; Kadish, K. M. *Anal. Chem.* **1985**, *57*, 1498−1501.
(21) Deshpande, R.; Jiang, L.; Schmidt, G.; Rakovan, J.; Wang, X.; Wheeler, K.; Wang, H. *Org. Lett.* **2009**, *11*, 4251−4253.
(22) Wagnert, L.; Berg, A.; Stavitski, E.; Berthold, T.; Kothe, G.; Goldberg, I.; Mahammed, A.; Simkhovich, L.; Gross, Z.; Levanon, H. *Appl. Magn. Reson.* **2006**, *30*, 591−604.
(23) Wagnert, L.; Rubin, R.; Berg, A.; Mahammed, A.; Gross, Z.; Levanon, H. *J. Phys. Chem. B* **2010**, *114*, 14303−14308.
(24) Kowalska, D.; Liu, X.; Tripathy, U.; Mahammed, A.; Gross, Z.; Hirayama, S.; Steer, R. P. *Inorg. Chem.* **2009**, *48*, 2670−2676.
(25) Liu, X.; Mahammed, A.; Tripathy, U.; Gross, Z.; Steer, R. P. *Chem. Phys. Lett.* **2008**, *459*, 113−118.
(26) Mason, J. *Multinuclear NMR*; Plenum Press: New York, 1987; p 369.
(27) Medforth, C. J.; Smith, K. M. *Tetrahedron Lett.* **1990**, *31*, 5583−5586.
(28) Medforth, C. J.; Berber, M. D.; Smith, K. M. *Tetrahedron Lett.* **1990**, *31*, 3719−3722.
(29) Medforth, C. J.; Senge, M. O.; Smith, K. M.; Sparks, L. D.; Shelnutt, J. A. *J. Am. Chem. Soc.* **1992**, *114*, 9859−9869.
(30) Ou, Z.; Shao, J.; Zhao, H.; Ohkubo, K.; Wasbotten, I. H.; Fukuzumi, S.; Ghosh, A.; Kadish, K. M. *J. Porphyrins Phthalocyanines* **2004**, *8*, 1236−1247.
(31) Kadish, K. M.; Adamian, V. A.; Van Caemelbecke, E.; Gueletii, E.; Will, S.; Erben, C.; Vogel, E. *J. Am. Chem. Soc.* **1998**, *120*, 11986−11993.
(32) Stefanelli, M.; Pomarico, G.; Tortora, L.; Nardis, S.; Fronczek, F. R.; McCandless, G. T.; Smith, K. M.; Manowong, M.; Fang, Y.; Chen, P.; Kadish, K. M.; Rosa, A.; Ricciardi, G.; Paolesse, R. *Inorg. Chem.* **2011**, *51*, 6928−6942.
(33) Simkhovich, L.; Mahammed, A.; Goldberg, L.; Gross, Z. *Chem.—Eur. J.* **2001**, *7*, 1041−1055.
(34) Kadish, K. M.; Ou, Z.; Adamian, V. A.; Guilard, R.; Gros, C. P.; Erben, C.; Will, S.; Vogel, E. *Inorg. Chem.* **2000**, *39*, 5675−5682.
(35) Stefanelli, M.; Mandoj, F.; Mastroianni, M.; Nardis, S.; Mohite, P.; Fronczek, F. R.; Smith, K. M.; Kadish, K. M.; Xiao, X.; Ou, Z.; Chen, P.; Paolesse, R. *Inorg. Chem.* **2011**, *50*, 8281−8292.
(36) *Organic Electrochemistry*, 4th ed.; Hammerich, O., Lund, H., Eds.; Marcel Dekker: New York, 2000; p 457.
(37) Chen, P.; Finikova, O. S.; Ou, Z.; Vinogradov, S. A; Kadish, K. M. *Inorg. Chem.* **2012**, *51*, 6200−6210.
(38) Ou, Z.; Shen, J.; Shao, J.; E, W.; Galezowski, M.; Gryko, D. T.; Kadish, K. M. *Inorg. Chem.* **2007**, *46*, 2775−2786.
(39) Shen, J.; Shao, J.; Ou, Z.; E, W.; Koszarna, B.; Gryko, D. T.; Kadish, K. M. *Inorg. Chem.* **2006**, *45*, 2251−2265.